The Astronomical Journal, 130:1231–1246, 2005 September

OPTICAL AND X-RAY STUDIES OF CHROMOSPHERICALLY ACTIVE STARS: FR CANCRI, HD 95559, AND LO PEGASI

J. C. Pandey,[1] K. P. Singh,[2] S. A. Drake,[3] and R. Sagar[1]

Received 2005 March 9; accepted 2005 May 31

ABSTRACT

We present a multiwavelength study of three chromospherically active stars, namely, FR Cnc (BD +16°1753), HD 95559, and LO Peg (BD +22°4409), including newly obtained optical photometry and low-resolution optical spectroscopy for FR Cnc, as well as archival IR and X-ray observations. The *BVR* photometry carried out from 2001 to 2004 has found significant photometric variability to be present in all three stars. For FR Cnc, a photometric period of 0.8267 ± 0.0004 days has been established. The strong variation in the phase and amplitude of the FR Cnc light curves when folded on this period implies the presence of evolving and migrating spots or spot groups on its surface. Two independent spots with migration periods of 0.97 and 0.93 yr, respectively, are inferred. The photometry of HD 95559 suggests the formation of a spot (group) during the interval of our observations. We infer the existence of two independent spots or groups in the photosphere of LO Peg, one of which has a migration period of 1.12 yr. The optical spectroscopy of FR Cnc carried out during 2002–2003 reveals the presence of strong and variable Ca II H and K, Hβ, and Hα emission features indicative of a high level of chromospheric activity. The value of 5.3 for the ratio of the excess emission in Hα to Hβ, $E_{\rm H\alpha}/E_{\rm H\beta}$, suggests that the chromospheric emission may arise from an extended off-limb region. We have searched for the presence of color excesses in the near-IR *JHK* bands of these stars using Two Micron All Sky Survey data, but none of them appear to have any significant color excess. We have also analyzed archival X-ray observations of HD 95559 and LO Peg carried out with the *ROSAT* observatory. The best-fit models to their X-ray spectra imply the presence of two coronal plasma components of differing temperatures and with subsolar metal abundances. The inferred emission measures and temperatures of these systems are similar to those found for other active dwarf stars. The kinematics of FR Cnc suggest that it is a very young (35–55 Myr) main-sequence star and a possible member of the IC 2391 supercluster. LO Peg also has young disk-type kinematics and has been previously suggested to be a member of the 100 Myr old Local Association (Pleiades moving group). The kinematics of HD 95559 indicate it is a possible member of the 600 Myr old Hyades supercluster.

Key words: binaries: general — stars: activity — stars: individual (FR Cancri, LO Pegasi, HD 95559) — X-rays: stars

1. INTRODUCTION

Differential rotation in late-type stars with convective envelopes drives a magnetic dynamo leading to strong chromospheric emission and the formation of a corona. The solar corona, although readily visible because of its proximity, is only about 10^{-6} of the solar photospheric emission. Rapidly rotating late-type stars, however, display extremely enhanced coronal activity when compared with that of the Sun. Strong X-ray and nonthermal radio emission in late-type stars are well-known indicators of enhanced coronal activity (Drake et al. 1992). Ayres and collaborators have shown (e.g., Ayres et al. 1995) that the emission from coronae ($T_e \sim 10^6$–10^7 K) and chromospheres ($T_e \sim 10^4$ K) are closely correlated, and thus stars with intense coronae will also have strong chromospheric emission. While many active stars have been identified as such through their above-average X-ray and radio emission, it is only through detailed optical photometric and spectroscopic studies that their activity can be classified into known types, such as the RS CVn, BY Draconis, and FK Comae classes. The common characteristic of all these various classes of active star, be they single stars or binaries, is rapid rotation; single, rapidly rotating stars either are young stars that have not yet lost most of their angular momentum or (in a few rare cases) are the results of the merger of a close binary system, while rapid rotation in close binaries is the natural result of spin-orbit tidal coupling and can occur even in middle-aged and/or old stars.

RS CVn types are binary systems that contain a hotter component with spectral type F–G and luminosity class V or IV, and a cooler component that is usually a subgiant or a giant K-type star (Hall 1976). RS CVn stars have been further subdivided into three groups according to their orbital period (P): short-period RS CVn ($P \leq 1$ day), classical RS CVn (1 day $< P \leq$ 14 days), and long-period systems usually containing at least one cool giant component ($P > 14$ days). BY Draconis type stars have properties similar to the RS CVn systems but consist of a late dKe- or dMe-type star with an orbital or rotational period in the range of ≈0.5 to ≈20 days. As originally defined by Bopp & Fekel (1977), BY Draconis types may include active, single main-sequence stars, as well as members of detached binary systems. (In the alternate definition of active binary systems of Fekel et al. [1986], there is no restriction on the spectral type of the companion star or on the orbital period for RS CVn binaries, except that the more active star is in an evolved evolutionary state, and systems with F- and G-type dwarf primaries are now classified as BY Draconis binaries rather than as a subtype of RS CVn systems). FK Comae stars are a rather rare class of apparently single, rapidly rotating late-type (G or K) giant stars that were first described by Bopp & Stencel (1981); the origin of these stars is still poorly understood, with the hypothesis

[1] Aryabhatta Research Institute of Observational Sciences, Naini Tal 263 129, India.
[2] Tata Institute of Fundamental Research, Bombay 400 005, India.
[3] Universities Space Research Association, 7501 Forbes Boulevard, Seabrook, MD 20706; and NASA Goddard Space Flight Center, Code 662, Greenbelt, MD 20771.

that they are the remnants of coalesced binaries being the most widely accepted. As a group, the late spectral type BY Draconis stars tend to more often exhibit Hα emission and more frequent flaring activity than the RS CVn systems, but this is probably mostly due to the greater contrast of their chromospheric emission lines with their weaker photospheric emission. Both RS CVn systems and BY Draconis binaries typically rotate synchronously with their orbital period, but there are more than 40 known systems (Glebocki & Stawikowski 1997) that are known to rotate asynchronously, e.g., the prototype K3.5 V+K3.5 V binary system BY Dra, which has a rotational period $P_{\rm rot}$ of 3.84 days and an orbital period of 5.98 days.

The soft (0.1–2.0 keV) X-ray luminosities ($L_{\rm X}$) of RS CVn systems are generally in the range of 10^{29}–10^{32} ergs s^{-1} (Drake et al. 1989), while BY Draconis stars tend to have $L_{\rm X} \approx 10^{29}$–$10^{30}$ ergs s^{-1} (Dempsey et al. 1993). In either case the values of $L_{\rm X}$ for these stars are $\approx 10^{2}$–10^{5} times the X-ray luminosity of the quiet Sun. The radio luminosity ($L_{6\,\rm cm}$) of RS CVn systems ranges from 10^{14} to 10^{17} ergs s^{-1} Hz^{-1} (Morris & Mutel 1988; Drake et al. 1989), while for the BY Draconis types it is typically 10^{12}–10^{15} ergs s^{-1} Hz^{-1} (Caillault et al. 1988; Güdel et al. 1993), much more than the quiet-Sun value of 3×10^{10} ergs s^{-1} Hz^{-1} in both cases. In this paper we present a detailed investigation based on our extensive optical observations and archival X-ray data of three chromospherically active stars selected on the basis of their strong X-ray and radio fluxes. These stars are FR Cnc, HD 95559, and LO Peg.

The star BD +16°1753 (MCC 527) first came to be noticed as a potential active star when it was identified as the likely optical counterpart of a soft X-ray source in the *Einstein* Slew Survey, 1ES 0829+15.9, with an observed X-ray flux of $\approx 10^{-11}$ ergs s^{-1} cm^{-2} (Elvis et al. 1992; Schachter et al. 1996). This X-ray source was rediscovered in the *ROSAT* All-Sky Survey (RASS) at a somewhat weaker (but more statistically significant) level of 2×10^{-12} ergs s^{-1} cm^{-2} and dubbed 1RXS J083230.9+154940 in the RASS Bright Source Catalogue (Voges et al. 1999). In the photometric notes annex of the *Hipparcos* catalog (Perryman et al. 1997), it was regarded as an unsolved variable star and given the name FR Cnc. It was recently classified as a BY Draconis type in the 74th Special Name-list of Variable Stars (Kazarovets et al. 1999). The implied X-ray luminosity of $(2-12) \times 10^{29}$ ergs s^{-1} and ratio of X-ray to bolometric luminosity $f_{\rm X}/f_{\rm bol} \geq 10^{-3.3}$ both show that FR Cnc has an active corona at or near the saturation limit of $f_{\rm X}/f_{\rm bol} \approx 10^{-3}$ (Schachter et al. 1996). Recently, Upgren et al. (2002) have given two measurements of the radial velocity of FR Cnc (see Table 6) that differ by only the order of the measurement error, and the authors thus conclude that it is not a binary system. A preliminary report on FR Cnc based on a limited subset of the data was presented by Pandey et al. (2002).

HD 95559 (BD +23°2287) has recently been shown to be a double-lined spectroscopic binary with an orbital period of 1.5260 days. With a photometric period of 1.5264 days, it is tightly synchronized to the orbital motion (Fekel & Henry 2000). Previous reports that this system has a 2.9 day photometric period (Jeffries et al. 1994a; Strassmeier et al. 2000) appear to have been the results of the detection of the 1 day alias of the 1.526 day orbital period. HD 95559 is a pair of K1 V stars with a Li-based age younger than the Hyades cluster. Fekel & Henry (2000) conclude that optical variability in this system is due to the rotational modulation of the star spots and thus identify it as belonging to the (binary) BY Draconis type.

LO Peg (BD +22°4409) is a single young K5 V–K7 V type star and is a member of the Local Association (Jeffries & Jewell 1993; Montes et al. 2001). It is an active star showing strong Hα and Ca II H and K emission lines (Jeffries et al. 1994b). Jeffries et al. (1994b) proposed six probable rotational periods and stated that the periods of 0.3841 and 0.42375 days are more likely. Subsequently, Robb & Cardinal (1995) eliminated completely the possibility of the 0.38417 day period. Evidence of an intense downflow of material and optical flaring on LO Peg have been presented by Eibe et al. (1999). Recently, Zuckerman et al. (2004) have identified LO Peg as a member of a group of $\sim$50 Myr old stars that partially surround the Sun.

The paper is organized as follows: In § 2 we describe the primary observational data sets that we have analyzed and the methods of data reduction. The optical light curve and the period analysis of the star FR Cnc are discussed in § 3. In § 4 we present the folded light and color curves of all three stars and provide an interpretation for the drift in phase of their wave minima. In § 5 we discuss the low-resolution optical spectra of FR Cnc that we have obtained. The *ROSAT* X-ray spectra of the stars HD 95559 and LO Peg are discussed in § 6, and § 7 contains a comparison of their X-ray properties with other similar stars. The physical parameters, *JHK* photometry, and kinematics of the stars FR Cnc, HD 95559, and LO Peg are described in §§ 8, 9, and 10, respectively, while we present our conclusions in § 11.

2. OBSERVATIONS AND DATA REDUCTIONS

2.1. *Optical Photometry*

FR Cnc, HD 95559, and LO Peg were observed in Johnson *B* and *V* and Cousins *R* filters from 2001 to 2004 at the State Observatory of Naini Tal (now renamed as the Aryabhatta Research Institute of Observational Sciences). The observations were made with the 104 cm Sampurnanand Telescope (SNT), to which a 2K × 2K CCD (field of view $\sim 13' \times 13'$) in the years 2001–2003 and a 1K × 1K CCD (field of view $\sim 6' \times 6'$) for 2003–2004 was attached. A log of the observations is given in Table 1. A number of CCD frames were taken on each night, with exposure times ranging from 10 to 120 s depending on the seeing conditions and the filter used. Several bias and twilight flat frames were taken during the observing runs. Bias subtraction, flat-fielding, and aperture photometry were performed using IRAF.[4] For each star, differential photometry in the sense of subtracting the comparison from the variable was done, as all the program, comparison, and check stars were in the same CCD frame.

UBVRI observations of FR Cnc along with that of the Landolt (1992) standard SA 98 region were obtained on 2004 February 22 for photometric calibration. The average magnitudes of FR Cnc in the *UBVRI* filters were 12.19 ± 0.02, 11.34 ± 0.01, 10.24 ± 0.01, 9.567 ± 0.009, and 8.89 ± 0.006, respectively. The present photometry is well matched to the Weis (1993) photometry. LO Peg was also observed for photometric calibration using PG 2213−006 standard fields (Landolt 1992) on 2002 October 3 in the *B*, *V*, *R*, and *I* bands. The corresponding average magnitudes were 9.86 ± 0.01, 8.82 ± 0.01, 8.22 ± 0.01, and 7.78 ± 0.01, respectively.

2.2. *Optical Spectroscopy*

Spectroscopic observations were carried out on 2002 November 15 and 2003 January 20–24 at the Vainu Bappu Observatory, Kavalur, with the OMR spectrograph fed by the 234 cm Vainu Bappu Telescope (VBT). The data were acquired with a 1K × 1K CCD camera of 24 μm square pixel size, covering a

[4] IRAF is distributed by the National Optical Astronomy Observatory.

TABLE 1
OBSERVATION LOG OF FR CNC, HD 95559, AND LO PEG

Object	Nights	Duration of Observations	Instrument	Telescope
		Optical Photometry		
FR Cnc	43	2001 Feb–2003 Jan	2K × 2K CCD	SNT
FR Cnc	10	2003 Dec–2004 Jan	1K × 1K CCD	SNT
FR Cnc	70[a]	1990 Mar–1992 Nov	...	*Hipparcos*
HD 95559	11	2001 Feb–2001 Apr	2K × 2K CCD	SNT
LO Peg	7	2001 Oct–2002 Oct	2K × 2K CCD	SNT
		Optical Spectroscopy		
FR Cnc	1	2002 Nov 15	OMR spectrograph (1K × 1K CCD)	VBT
FR Cnc	5	2003 Jan 20–24	OMR spectrograph (1K × 1K CCD)	VBT

[a] Total number of measurements made by *Hipparcos*.

range of ~1200 Å and having a dispersion of 1.25 Å pixel^{-1}. A signal-to-noise ratio between 20 and 30 was achieved. During these observations we took 10 spectra of FR Cnc in the Hα region, 6 in the Hβ region, and 5 in the Ca II H and K region. A total of 21 spectra were thus taken. HD 26795, a K3 V type star, was observed as the standard.

The spectra have been extracted using the standard reduction procedures in the IRAF packages (bias subtraction, flat-fielding, extraction of the spectrum, and wavelength calibration using arc lamps). The spectral resolution was determined by using emission lines of arc lamps taken on the same nights. Spectral resolution ($\delta\lambda$) of 2.7 Å at 6300 Å and 3.7 Å at 4000 Å was achieved. All the spectra were normalized to the continuum, and equivalent widths for emission lines were computed using the IRAF task *splot*. The errors in the measurements of the equivalent widths of the Hα, Hβ, and Ca II H and K lines were computed by measuring the equivalent widths of four moderate absorption features at 6494, 6163, 6122, and 6103 Å in each spectrum. The standard deviation for each absorption feature was computed from the 10 spectra available. The mean of the standard deviations thus obtained was 0.04 Å and was taken as the error in the measurement of the equivalent widths of all the absorption, as well as of the emission-line features (see also Padmakar et al. 2000).

2.3. *X-Ray*

The stars HD 95559 and LO Peg were observed serendipitously in pointed observations of the *ROSAT* PSPC. This instrument had an energy range of 0.1–2.4 keV with a rather low spectral resolution ($\Delta E/E \approx 0.42$ at 1 keV). A full description of the X-ray telescope and detectors can be found in Trümper (1983) and Pfeffermann et al. (1987). The *ROSAT* X-ray data for these two stars were obtained from the High Energy Astrophysics Science Archive Research Center (HEASARC). The *ROSAT* observational parameters are given in Table 2. LO Peg was observed on two occasions, the first on 1993 November 11–13 and the second a month later on 1993 December 7–8, while the HD 95559 observation consisted of two short exposures in 1993 June separated by a week. (FR Cnc was not observed in any of the pointings made by *ROSAT*, but it was, however, detected in the RASS phase, as has already been mentioned in § 1.) HD 95559 and LO Peg were offset from the center of the PSPC field by 38.′4 and 0.′31, respectively. Spectra of both stars were accumulated from on-source counts obtained from circular regions on the sky centered on the X-ray peaks. The background was accumulated from several neighboring regions at nearly the same offset as the source.

3. LIGHT CURVES AND PERIOD ANALYSIS OF FR CNC

3.1. *Present Light Curve*

We obtained nine light curves, with each light curve corresponding to an observational run that was nearly continuous. Figure 1 shows the light curves of FR Cnc for each epoch. The mean epochs of the light curves, observed maxima ($\Delta V_{\max}$) and minima ($\Delta V_{\min}$) in the V band, peak-to-peak amplitudes ($\Delta V = \Delta V_{\max} - \Delta V_{\min}$), and phase minima ($\theta_{\min}$) are listed in Table 3. The quantity $\theta_{\min}$ was determined by a linear least-squares fitting of the second-order polynomial at the minimum of each light curve. It appears that the shapes and the amplitudes of the light curves were changing during the observing season.

During the observing season 2001–2003 for the star FR Cnc, the comparison and check stars were TYC 1392 2110 1 (written as S1 below) and USNO-A2.0 1050-05766589 (C below), respectively. BD +16°1751 (S2 below), of spectral type G0, was taken as the comparison star during the observing season 2003–2004. The difference between the mean of (S2 − C) and the mean of (S1 − C) in each *BVR* filter was added to the *BVR* data of the 2003–2004 season before plotting. No significant light variation was detected between the different measures of comparison and check stars (ΔV_c; see the bottom plots in each panel of Fig. 3), indicating that the comparison stars were constant

TABLE 2
X-RAY OBSERVATIONS FROM *ROSAT* OF HD 95559 AND LO PEG

Source	Observation ID	Duration of Observations	Exposure (s)	Count Rate (counts s^{-1})	Offset (arcmin)
HD 95559	rp200987n00	1993 Jun 2–9	4874	0.62 ± 0.02	38.4
LO Peg	rp201753n00	1993 Nov 11–13	5968	1.07 ± 0.01	0.31
LO Peg	rp201753a01	1993 Dec 7–8	14012	1.02 ± 0.01	0.31

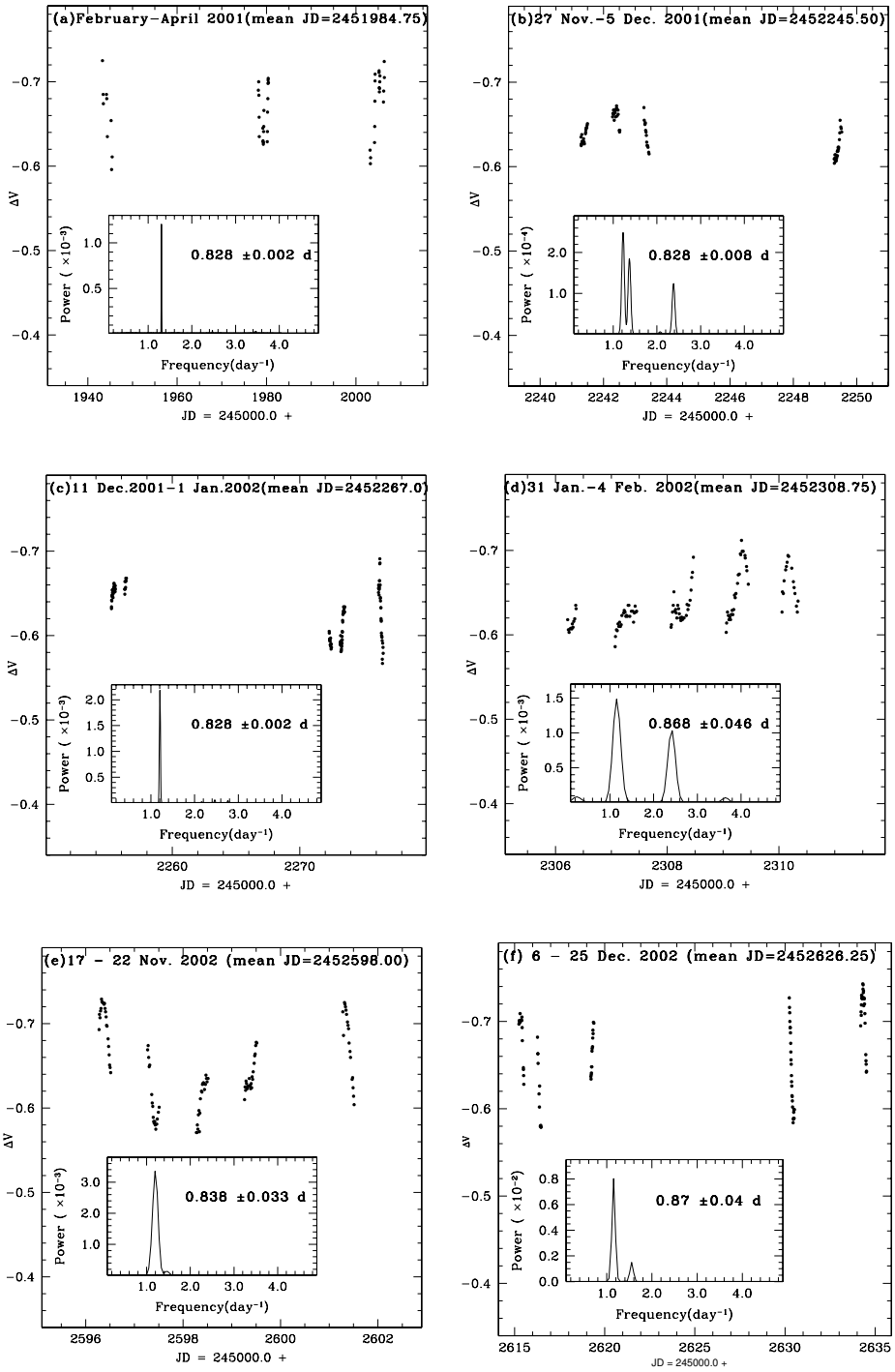

FIG. 1.—Light curves and corresponding CLEANed power density spectra (*insets*) of FR Cnc at different epochs. The epoch is mentioned at the top of each panel, and the period is written at the top of each inset. Panel *j* shows the *Hipparcos* light curve along with its power spectrum.

during those observations. The nightly mean of the standard deviation (σ) of different measures of the comparison and check stars in the *B*, *V*, and *R* filters was 0.007, 0.007, and 0.008 mag, respectively. Similarly, σ determined for $\Delta(B-V)_c$ and $\Delta(V-R)_c$ was 0.006 and 0.01 mag, respectively.

Large gaps in the data set led to complications in the interpretation of the power density spectrum, as the true frequencies of the source were further modulated by the irregular and infrequent sampling defined by the window function of the data. Therefore, the calculation of the dirty power density spectrum from the light curve was followed by deconvolution of the window function from the data using the one-dimensional CLEAN (Roberts et al. 1987) algorithm in Starlink's PERIOD package, where we have assumed a quasi-sinusoidal light curve. The power spectrum picks out the rotation period despite the noise and the fact that the light curve is not exactly sinusoidal (Bailer-Jones & Mundt 2001). The uncertainty in the period determination is set by the finite resolution of the power spectrum. This is determined as $P^2/(2t_{\max})$, where P is the period and $t_{\max}$ is the duration of the observation (Roberts et al. 1987). The CLEANed power spectra presented here were obtained after 100 iterations with a loop gain of 0.1. Data for each epoch were analyzed separately for the periodicity by using the CLEAN algorithm. Inset in each panel of Figure 1 is the corresponding CLEANed power spectrum. The

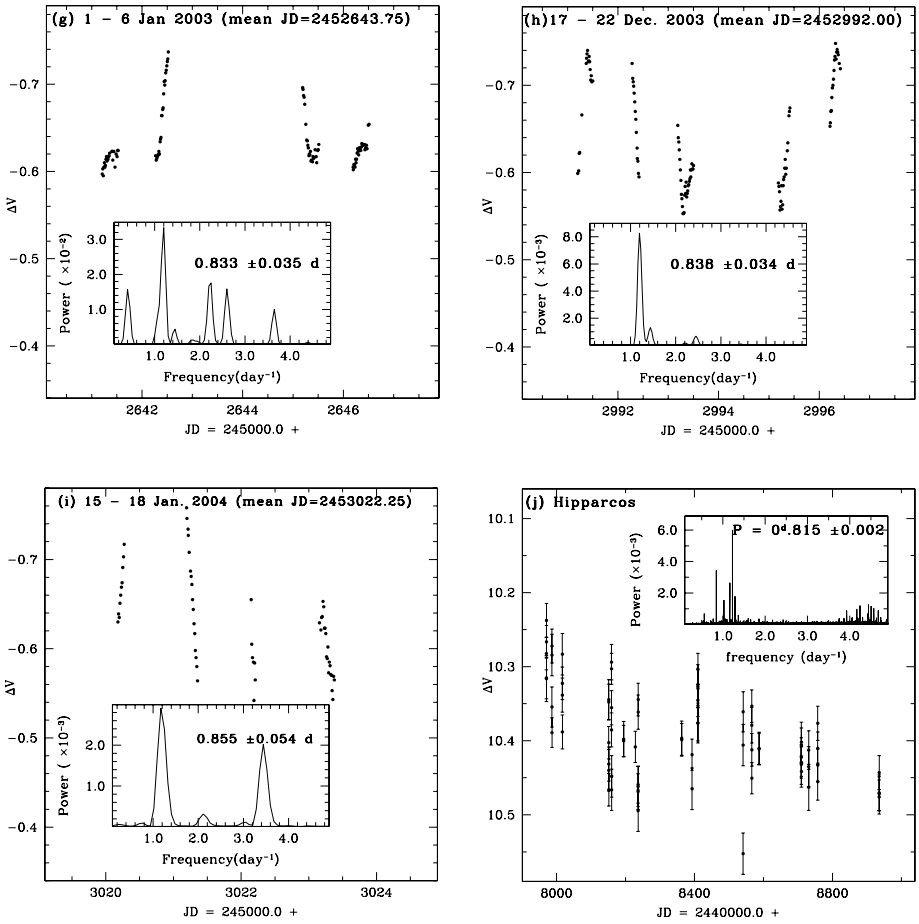

FIG. 1.—*Continued*

TABLE 3
PHOTOMETRY OF FR CNC, HD 95559, AND LO PEG

MEAN EPOCH (2,400,000.0+)	AMPLITUDE ΔV	ΔV_{max}	ΔV_{min}	PHASE MINIMA I	PHASE MINIMA II
		FR Cnc			
51,984.75	0.106	−0.716	−0.610	0.33	0.75
52,245.50	0.063	−0.670	−0.607	0.29	0.66
52,267.00	0.108	−0.683	−0.575	0.27	...
52,308.75	0.100	−0.697	−0.597	0.23	0.58
52,598.00	0.153	−0.725	−0.572	0.44	0.75
52,626.25	0.158[a]	−0.738	−0.580	...	...
52,643.75	0.128[a]	−0.728	−0.600	0.39	0.62
52,992.00	0.210	−0.721	−0.511	0.25	0.54
53,022.25	0.181[a]	−0.736	−0.555	0.21	0.53
		HD 95559			
51,945.40	0.051	−0.435	−0.384	0.00	...
52,003.80	0.076	−0.481	−0.405	0.00	0.53
		LO Peg			
52,190.80	0.081	−0.483	−0.402	0.50	...
52,548.00	0.050	−0.495	−0.445	0.66	...

[a] Because certain phases were not covered fully during these observations, minima and/or maxima at these epochs could not be determined accurately.

epoch and the period are mentioned inside each panel of Figure 1. The period is found to be constant, within the uncertainty, for each epoch.

The entire data set was also analyzed as a whole using the CLEAN algorithm to improve the period determination. Figure 2 (*top*) shows the discrete power spectra, with the corresponding window and CLEANed power spectra shown in the middle and bottom panels. The highest peak in the CLEANed power spectrum corresponds to a period of 0.8267 ± 0.0004 days.

3.2. *Hipparcos Light Curve*

The light curve based on the *Hipparcos* photometric data is shown in Figure 1*j*. The total number of measurements with *Hipparcos* was 70 during 3 yr (1990 March–1992 November) of observations. We have also analyzed the *Hipparcos* data using the same algorithm as used for our photometric data. The CLEANed power spectrum is shown in the inset of Figure 1*j*. The highest peak here corresponds to a period of 0.815 ± 0.002 days, which is close to the period determined from the present data.

4. FOLDED LIGHT AND COLOR CURVES

4.1. *FR Cnc*

The data were folded using a period of 0.8267 days and an arbitrary epoch of JD $= 2,451,943.1980$. Figure 3 shows plots of ΔV_c, ΔB, ΔV, ΔR, $\Delta(B-V)$, and $\Delta(V-R)$ as functions of phase at different epochs. The mean epoch is mentioned at the top of each panel of Figure 3. As can be seen from Figure 3, the

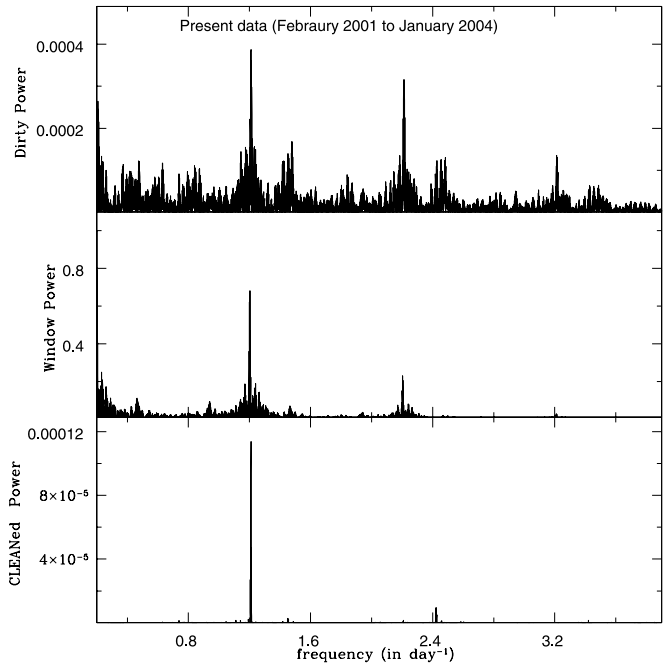

FIG. 2.—Power spectra of FR Cnc from the entire photometric data set taken during 2001–2004. *Top*, Dirty power density spectrum; *middle*, corresponding window power; *bottom*, CLEANed power density spectrum.

phase coverage is fair to reasonably good in most of the light curves.

The value of $\Delta V_{\max}$ was nearly constant during most of the epochs, indicating that the brightness of the unspotted photosphere was constant from epoch to epoch. During epoch b it went to its minimum value. A smaller variation ($\Delta V = 0.063$ mag) during this epoch was probably associated with a continuous reduction of the spot coverage. The light curve during epoch b has two maxima, whereas during epoch c it has one flat maximum and one minimum, indicating the formation of a new group of spots that further separate into two groups of spots during epochs d and e. An increase in the amplitude by 0.05 mag during epoch e indicates an increase in the spot coverage on the surface of the star that remained constant during epoch f. However, the poor phase coverage during epochs f, g, and i does not allow us to follow this progress of spots properly. The activity level in our observation became very high during epoch h, in which the amplitude of variation became 0.21 mag and appeared to remain the same during epoch i. Variable sizes of the spot (or group of spots) are indicated by the variable depth of the light minimum in the light curves. The minimum of the light changed by 0.1 mag from epoch a to h (see Table 3).

When comparing the light curves of FR Cnc from epoch a to i, a shift in the phase of the minimum and a variable amplitude are quite evident. Such cycle-to-cycle variations of both the amplitude and phase of the minimum have been seen for some rapidly rotating stars such as LO Peg (Dal & Tas 2003), Speedy Mic (Barnes et al. 2001), AB Dor (Bos 1994; Donati & Collier Cameron 1997), and PZ Tel (Innis et al. 1990).

Variation in the color of the star is correlated with its magnitude, i.e., the star becomes redder when fainter and bluer when brighter, supporting the starspot hypothesis. The significance of correlation has been calculated by determining the linear correlation coefficient r between the magnitude and the colors. The value of r between V and $(B - V)$, V and $(V - R)$, and $(B - V)$ and $(V - R)$ was found to be 0.11, 0.35, and 0.581 with the corresponding probability of no correlation being 0.00181, 1.51×10^{-25}, and 0, respectively.

4.1.1. *Phase of the Light Minimum*

The phase minimum of light ($\theta_{\min}$) for the nine light curves in the V band were plotted against the mean epoch listed in Table 3 and are shown in Figure 4 (*left*). To illustrate the spot motions over several longitudinal cycles, we define the longitude as longitude $+ n \times 360^\circ$ or $\theta_{\min} + n \times 1$, where n is the cycle number. The phases of the light minima directly indicate the mean longitude of the dominant groups of the spots. The presence of two spots is clearly established by two well-separated straight lines. The spots are closer to each other during epoch g, with a longitudinal separation of $\sim 83^\circ$. Both spots are visible during all epochs except epoch c. The poor phase coverage during epoch f prevented us from establishing the presence of the second spot. It is interesting to see the variable separation of the two spots. This could be due to the different latitudinal positions of the two spots and the presence of differential rotation in the star. Because of differential rotation, spots at different latitudes would give rise to a different migration rate for the associated $\theta_{\min}$ (Raveendran & Mohin 1995).

The following relation was fitted to the data by the method of least squares:

$$\theta_{\min} = \omega(t - t_0) + \theta_0, \tag{1}$$

where $\omega = 2\pi/P$ is the angular velocity of the spot or the rate of phase shift (deg day^{-1}), P is the corresponding period in days, t is the time in days, t_0 is the reference time, and θ_0 is the reference spot longitude in degrees. Applying the above relation, the rate of phase shift for spots A and B is determined to be $1\overset{\circ}{.}02 \pm 0\overset{\circ}{.}02$ day^{-1} and $1\overset{\circ}{.}06 \pm 0\overset{\circ}{.}02$ day^{-1}, respectively. The corresponding migration period for spots A and B is found to be 0.97 ± 0.03 and 0.93 ± 0.02 yr, respectively. These migration periods, being so close to each other, indicate that the spots that are located at different longitudes rotate with almost the same angular velocity. It thus appears that the observed phase minima of FR Cnc are well arranged in two permanent strips with approximately the same slope (i.e., same migration period), which can be interpreted as two long-lived active longitudes.

4.2. *HD 95559*

Stars HD 95467 and BD $+33^\circ 2294$ were observed for the differential photometry of the program star HD 95559. The data were folded using the following ephemeris for HD 95559:

$$\mathrm{JD} = 2,450,359.094 + 1.52599775E,$$

where the epoch corresponds to a time when the more massive star is in front of the less massive star and the period is the spectroscopic orbital period (Fekel & Henry 2000). Variations in the BVR magnitude and colors of the program star with respect to the comparison star are shown in Figure 5. The nightly mean σ of the different measures of the comparison and check stars was determined to be 0.006 in each B and V filter and 0.007 in the R filter. The comparison star was constant during the observations, as shown in the bottom plots in each panel of Figure 5. We have divided our observations into two epochs, namely, epoch a (2001 February 3–5) and epoch b (2001 March 31–April 7). The amplitudes and phases of the minima for mean epochs of the observations of this star are shown in Table 3.

It is interesting to examine the light curves of HD 95559 during the observing season of 2001. During epoch a the light curve

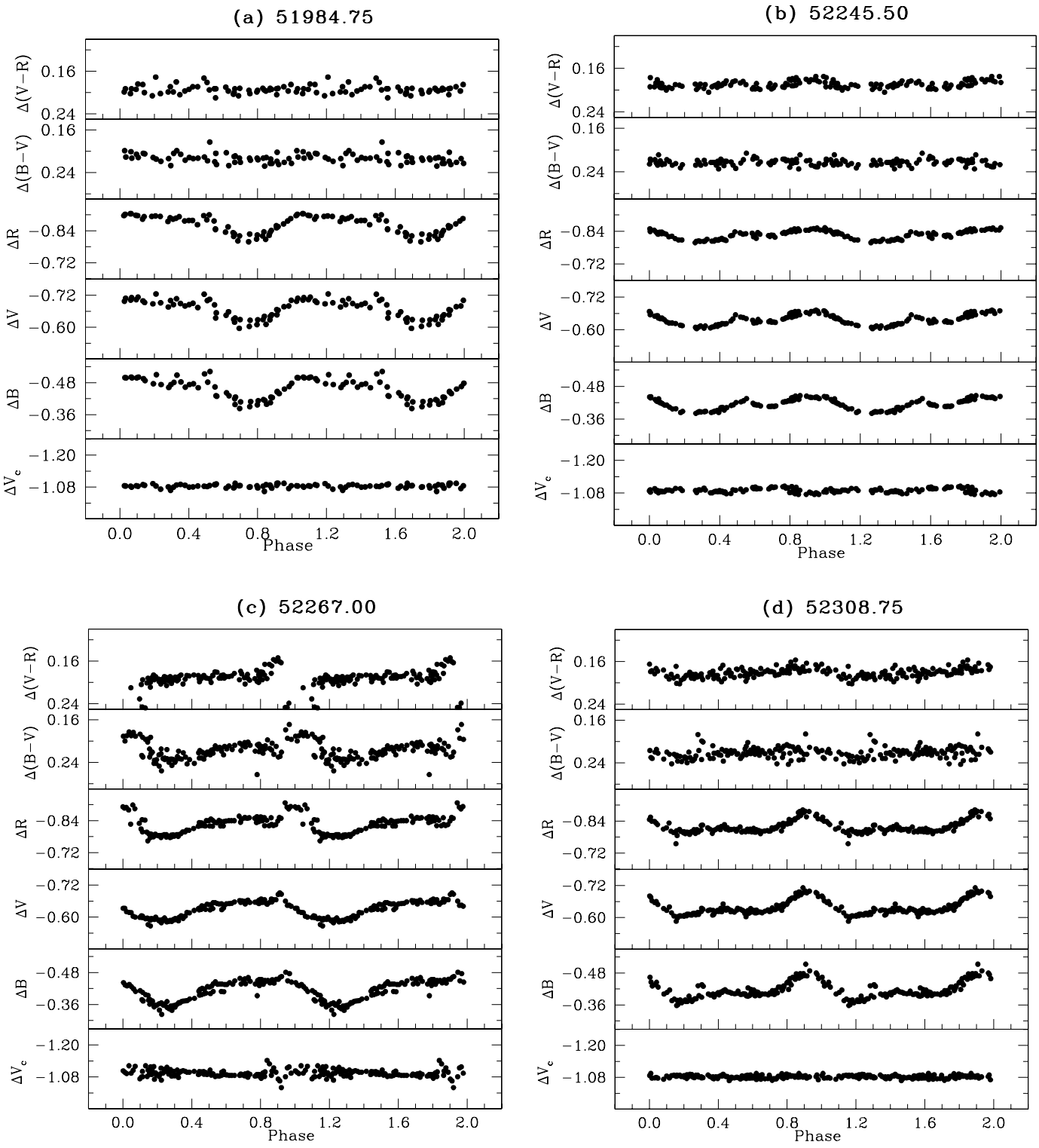

FIG. 3.—V_c, B, V, and R light curves and $(B - V)$ and $(V - R)$ color curves of FR Cnc, folded using a period of 0.8267 days and shown for nine different epochs. The epoch (JD = 2,400,000.0+) is marked at the top of each panel. The bottom plot in each panel represents the differences between the comparison star (TYC 1392 2120 1 for *a*–*g* and BD +16°1751 for *h* and *i*) and the check star (USNO-A2.0 1050-05766589).

has a flat-topped maximum and only one minimum (Fig. 5*a*). During epoch b that flat-topped maximum develops into a minimum at a phase of 0.5. At the same time, the amplitude of the variation increases by 0.025 mag. The position of the minimum during epoch a, however, does not change from the phase 0.0. This directly indicates the formation of a new group of spots at phase 0.5. Light curves of HD 95559 during the observing season 1995–1997 had only one minimum and a sharp maximum (Fekel & Henry 2000).

It appears that the colors remain nearly constant during our observations in HD 95559. A larger amount of scatter is, however, seen during epoch b. This may be due to the formation of the new group of spots on the surface of the active star. The lack of a brightness-color relation may be due to the presence of bright

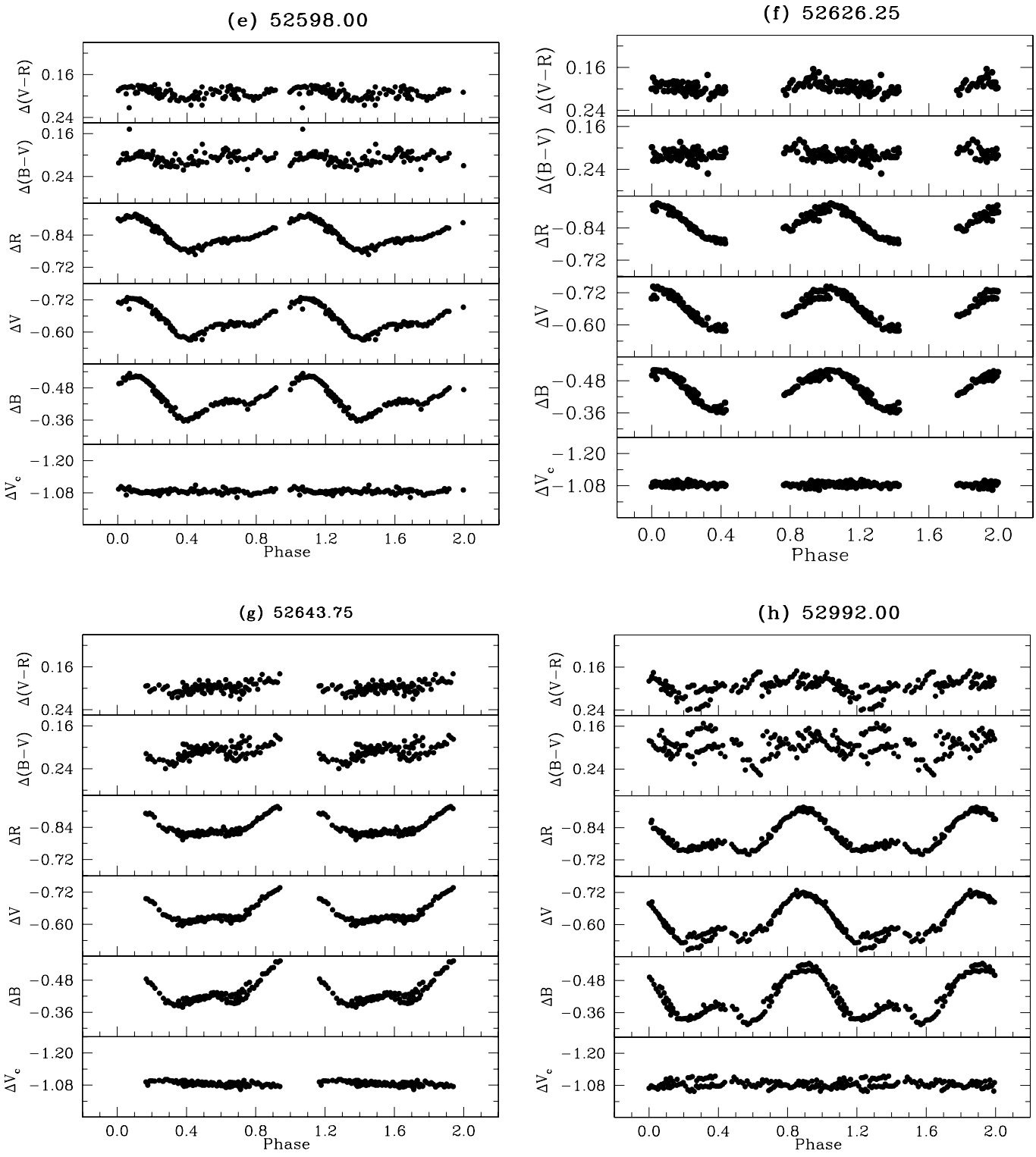

FIG. 3.—*Continued*

faculae or plages, such as regions accompanied by dark spots in either or both components of this binary system.

4.3. *LO Peg*

Photometric data of LO Peg were folded using the following ephemeris as given by Dal & Tas (2003):

$$\mathrm{HJD} = 2,448,869.93 + 0.42375E.$$

The folded light curves are shown in Figure 6. The observations, separated by a year, were divided into two different epochs, namely, epochs a and b. Epoch a has observations from 2001 September 28 to October 15, and epoch b has observations from 2002 September 28 to October 3. The epoch b observations partly coincide with one set of observations (2002 October 1–31) of Dal & Tas (2003). Table 3 shows the parameters determined from the light curves of LO Peg. The phase minimum computed from our photometry at epoch b differs by 0.26 from that of Dal & Tas

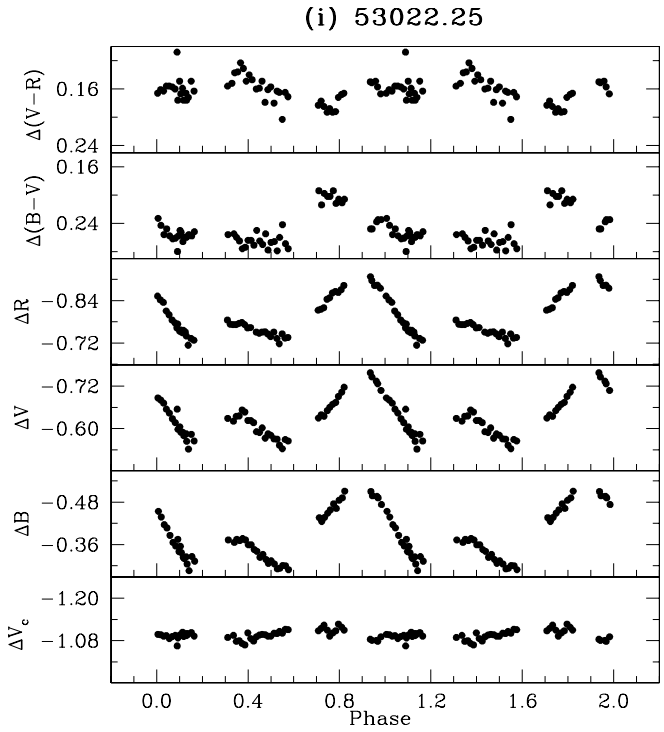

FIG. 3.—*Continued*

(2003). This may be due to the larger span of their observations, as the phase minimum changed significantly within a couple of rotational periods, probably as a result of a change in the spot configuration. As in the case of FR Cnc, no two light curves of LO Peg are similar in shape, size, or amplitude, which is seen quite commonly in the BY Draconis type of star.

A plot of the phase minima as a function of the mean epoch of the observations of LO Peg is shown in Figure 4 (*right*). The filled circles represent the observations made by Dal & Tas (2003), and the triangles represent our observations. Two large groups of spots are clearly seen. We have fitted equation (1) with the linear least-squares method for the spot group A and have computed the rate of phase shift. The open circle in Figure 4 (*right*) was not used in the fitting. The rate of the phase shift for the spot group A was determined to be $0\overset{\circ}{.}85 \pm 0\overset{\circ}{.}03$ day^{-1}. The corresponding migration period is 1.12 ± 0.05 yr.

From Figure 6 it is clear that the color curves are strongly correlated with light curves, i.e., bluer at light maximum and redder at light minimum. This indicates that the variability is due to the dark spots present on the surface of the star.

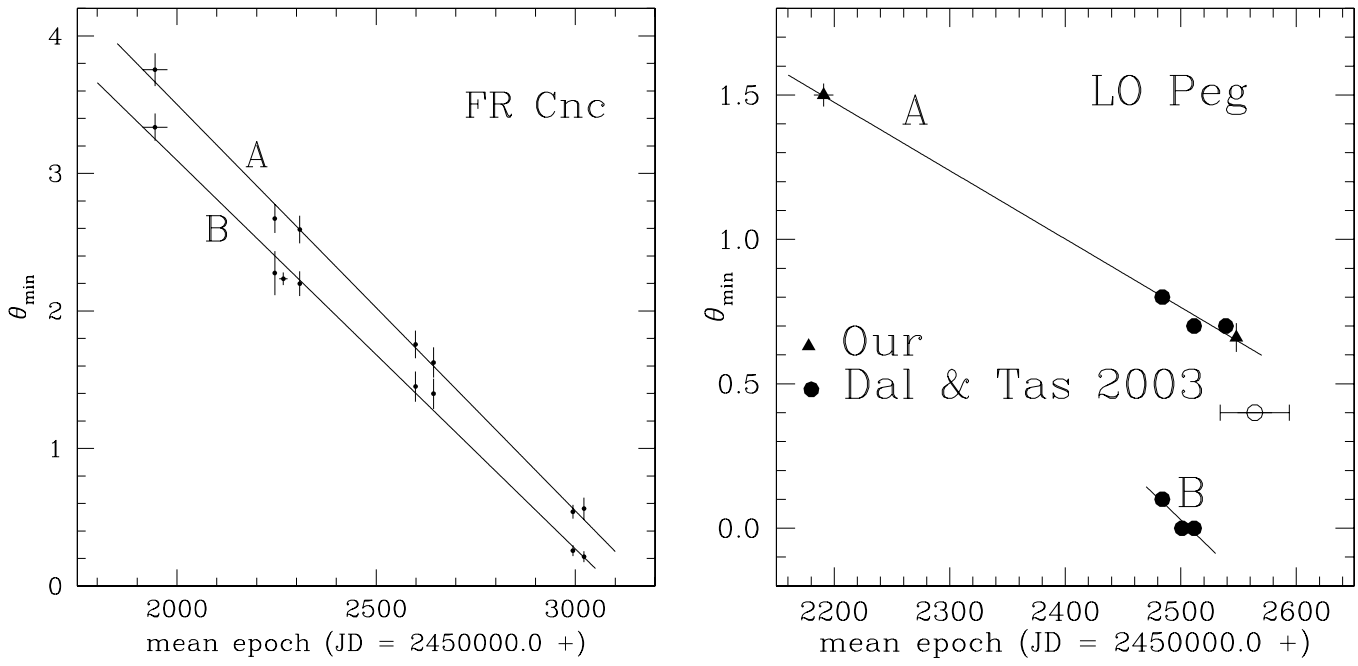

FIG. 4.—Mean epoch vs. the phase minimum of light for FR Cnc (*left*) and LO Peg (*right*). The open circle in the right panel was not used in the fitting. Vertical bars show the associated errors in the determination of phase minima, and the horizontal bar shows the length of the epoch.

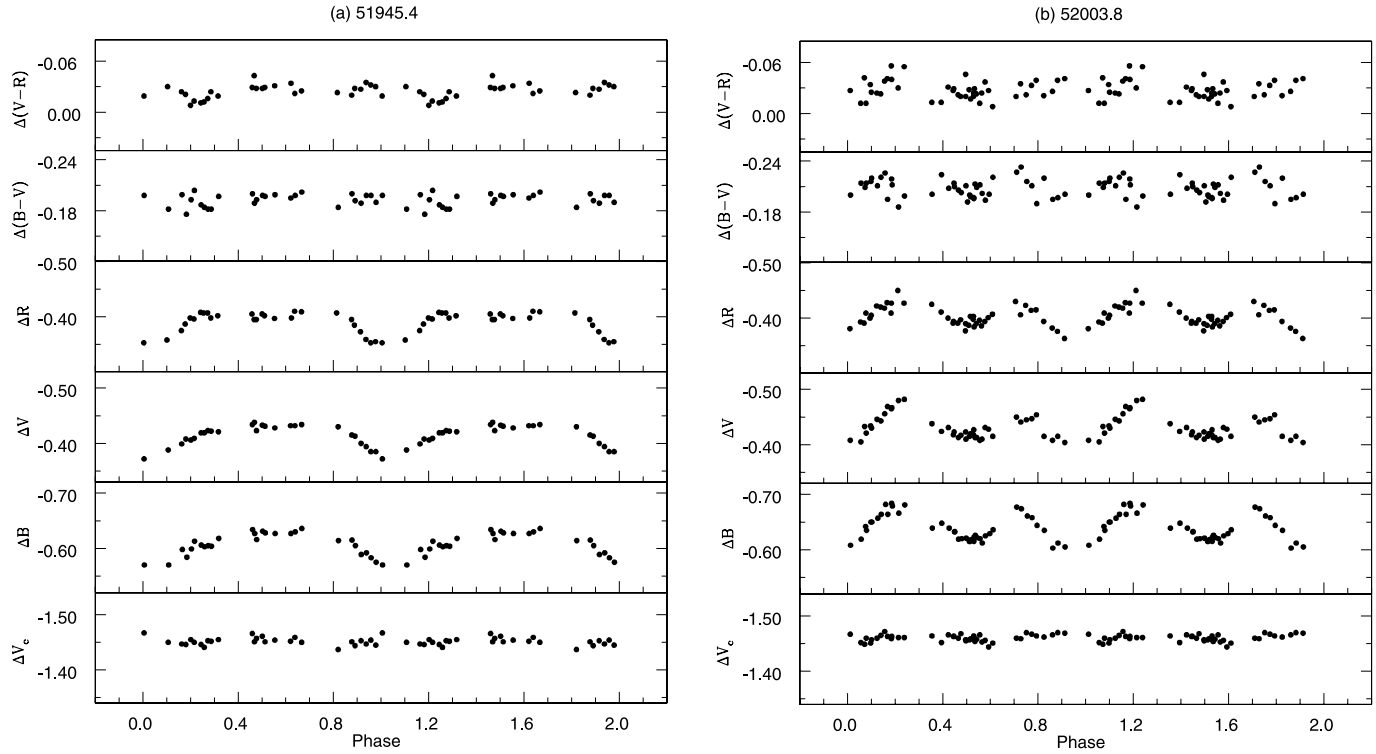

FIG. 5.—V_c, B, V, and R light curves and $(B-V)$ and $(V-R)$ color curves of HD 95559, folded using a period of 1.52599775 days and shown for two different epochs. The epoch (JD $= 2,400,000.0+$) is marked at the top of each panel. The bottom plot in each panel represents the differences between the comparison star (HD 95467) and the check star (BD +33°2294).

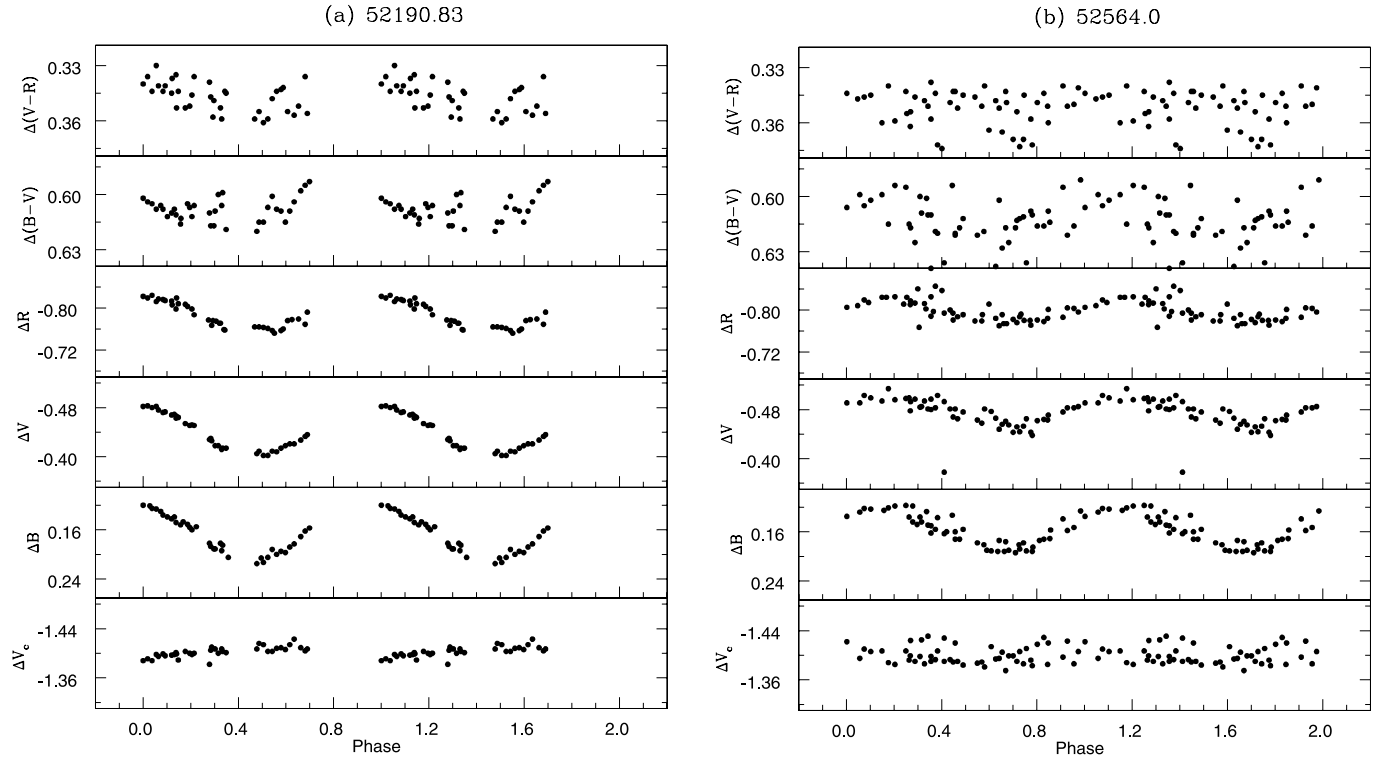

FIG. 6.—V_c, B, V, and R light curves and $(B-V)$ and $(V-R)$ color curves of LO Peg, folded using a period of 0.42375 days and shown for two different epochs. The epoch marked at the top of each panel is JD $= 2,400,000.0+$. The bottom plot in each panel represents the differences between the comparison star (BD +22°4405) and the check star (USNO-B1.0 1133-0542608).

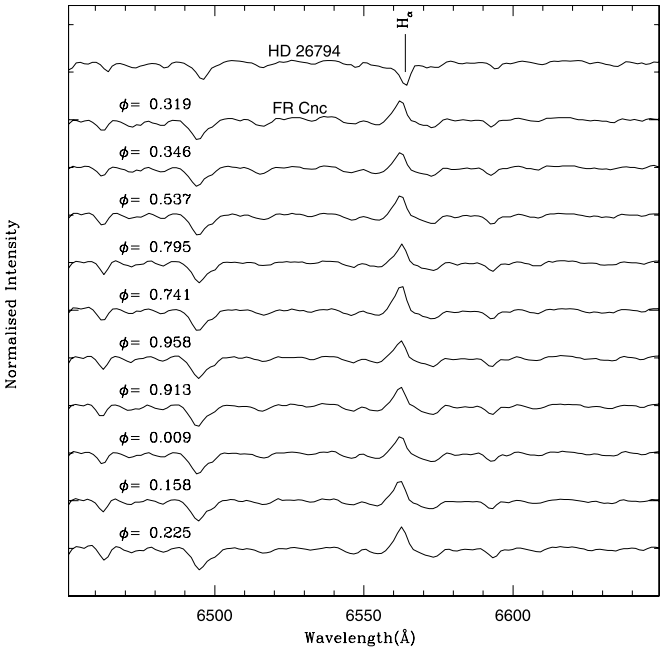

FIG. 7.—Hα spectra of FR Cnc and the comparison star HD 26794. The phase is mentioned at the top of each spectrum.

TABLE 4

Ca II H AND K, Hα, AND Hβ DATA FOR FR CNC

		EQUIVALENT WIDTHS (Å)			
JD (2,400,000+)	PHASE	Ca II K	Ca II H	H α	Hβ
52,594.400	0.73	6.45	5.70	...	...
52,594.431	0.77	5.39	4.58	...	...
52,660.197	0.32	...	...	1.51	...
52,660.220	0.35	...	...	1.21	...
52,660.463	0.64	...	...	...	0.40
52,660.486	0.67	...	...	...	0.33
52,661.204	0.54	...	...	1.498	...
52,661.251	0.59	5.19	4.59	...	...
52,661.417	0.79	...	...	1.32	...
52,661.446	0.83	...	...	...	0.36
52,662.199	0.74	...	...	1.82	...
52,662.248	0.80	5.06	4.86	...	...
52,662.379	0.96	...	...	1.39	...
52,662.452	0.05	...	...	...	0.40
52,663.168	0.91	...	...	1.55	...
52,663.217	0.97	5.67	4.22	...	...
52,663.247	0.01	...	...	1.36	...
52,663.371	0.16	...	...	1.64	...
52,663.422	0.22	...	...	...	0.31
52,664.253	0.23	...	...	1.62	...
52,664.508	0.53	...	...	...	0.31

We have also checked whether the comparison star (BD +22°4405) is variable. Star TYC 2188 1288 1 was used as a check star. The σ was computed between the different measures of the comparison and check stars. The nightly means of σ were 0.010, 0.009, and 0.007 in the *B*, *V*, and *R* filters, respectively. The bottom plots in each panel of Figure 6 show the different measures of the comparison and check stars and indicate that the comparison stars were indeed constant during the observations.

5. CHROMOSPHERIC EMISSION LINES OF FR CNC

In late-type dwarfs, Hα emission is a good indicator of chromospheric activity. It has been suggested that the detection of Hα emission above the continuum or even a filled-in emission is sufficient to indicate that a K–M dwarf is a BY Draconis variable (Bopp et al. 1981). The spectrum of FR Cnc in the Hα region is shown in Figure 7. The spectrum of HD 26794 (V = 8.81 mag and spectral type K3 V) is also shown in Figure 7 for comparison. Hα is in emission at all phases in FR Cnc. The measured equivalent widths of the Hα emission feature and the corresponding JDs and phases of FR Cnc are listed in Table 4. The phase is determined using a photometric period of 0.8267 days and an epoch of JD = 2,451,943.1980 for phase 0. The equivalent width is seen to vary from 1.2 to 1.8 Å. Such a significant change in the Hα profiles and the equivalent width on a timescale as short as a few hours has also been reported for the active K5 V star LO Peg (Jeffries et al. 1994b).

Hβ emission in late-type stars is another indicator of enhanced chromospheric activity. Figure 8 shows the spectra of FR Cnc and the comparison star HD 26794 in the Hβ region. Hβ is seen clearly in emission, while it is in absorption in the comparison star. The ratio of excess emission $E_{\mathrm{H}\alpha}/E_{\mathrm{H}\beta}$ with the correction given by Hall & Ramcey (1992) was also calculated for FR Cnc as

$$\frac{E_{\mathrm{H}\alpha}}{E_{\mathrm{H}\beta}} = \frac{\mathrm{EW(H}\alpha)}{\mathrm{EW(H}\beta)} \times 0.2444 \times 2.512^{(B-R)}.$$

This yields a value of 5.34 for the mean values of the equivalent widths of Hα and Hβ. According to Hall & Ramcey (1992), values of $E_{\mathrm{H}\alpha}/E_{\mathrm{H}\beta} > 3$ are indicative of the line emission likely arising from an extended region viewed off the limb, perhaps a stellar prominence.

Figure 9 shows a comparison of the spectrum of FR Cnc with that of HD 26794 in the region near the Ca II H and K lines. One can see that these lines have strong central emission components in the spectra of FR Cnc because of its active chromosphere. The spectrum of the Ca II H and K region taken on 2002 November 15

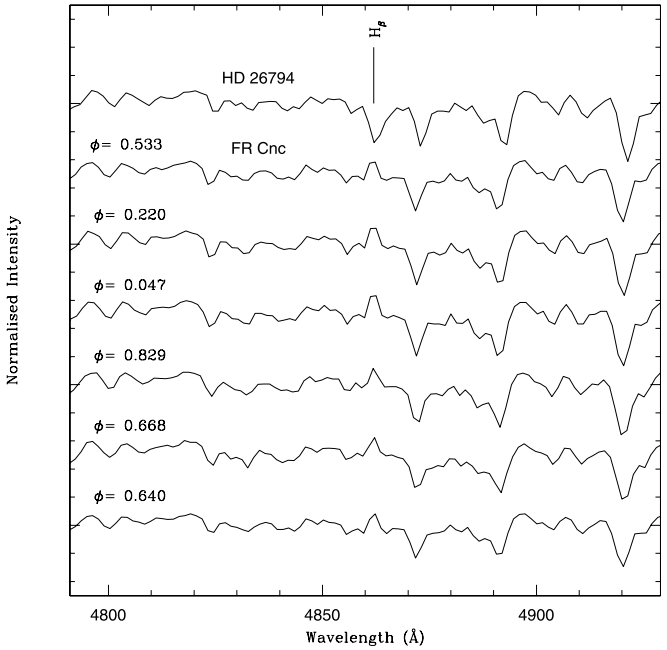

FIG. 8.—Spectra of FR Cnc showing Hβ in emission, with the spectrum of HD 26794 showing Hβ in absorption. The phase is mentioned at the top of each spectrum of FR Cnc.

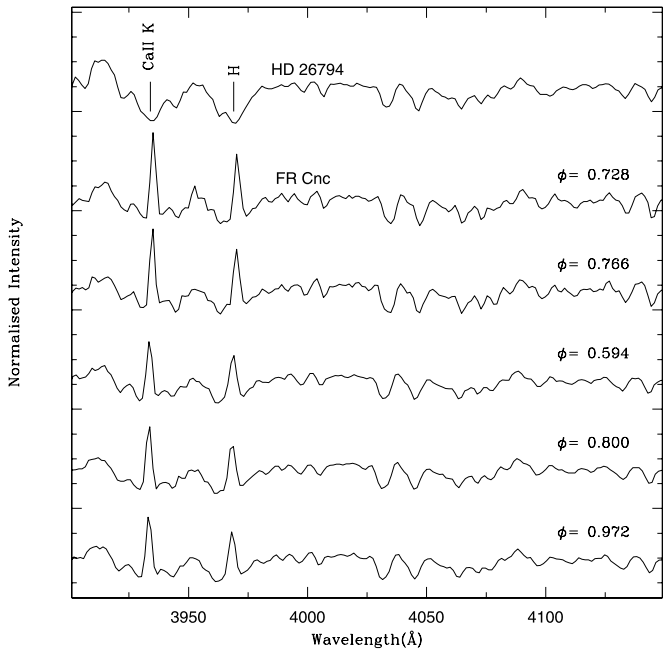

FIG. 9.—Spectra of FR Cnc and the comparison star HD 26794 near the Ca II region. The phase is mentioned at the top right of each spectrum of FR Cnc.

($\phi = 0.72$ and 0.76 cycles) was obtained close to photometric epoch e (Fig. 3*e*). The photometric light minima during this epoch are at phases of 0.44 and 0.75. The equivalent widths of the Ca II H and K lines in the 2002 November 15 spectra were found to be at a maximum during the photometric light minimum. Such a correlation is seen quite commonly among chromospherically active stars and is typically interpreted as evidence that, as in the solar case, the plage regions responsible for the Ca II emission are adjacent to the spotted regions responsible for the photometric modulation.

The equivalent widths of the Hα and Ca II H and K lines in FR Cnc are in the range of 1.2–1.8 and 4.2–6.4 Å, respectively. This is similar to the equivalent width found in most BY Draconis type stars (see, e.g., Bopp 1987).

6. X-RAY SPECTRA

The X-ray spectra of HD 95559 and LO Peg are shown in the left and right panels of Figure 10, respectively. We created response matrices based on the available off-axis calibration of the PSPC and using the appropriate ancillary response files. We used the XSPEC (ver. 11.2) spectral analysis package to fit the data with the spectral model for thermal equilibrium plasma known as the Mewe-Kaastra-Liedahl (MEKAL) model (Liedahl et al. 1995; Mewe et al. 1995). The background-subtracted X-ray spectra were fitted with one-temperature (1T) and two-temperature (2T) plasma models assuming the solar photospheric abundances given in Anders & Grevesse (1989) and allowing the abundance of every element other than H to vary by a common factor relative to their solar (photospheric) values. In each of the above models we assumed that interstellar absorption follows the absorption cross sections given by Morrison & McCammon (1983), and we allowed the total intervening hydrogen column density $N_{\rm H}$ to vary freely. We have also fitted the X-ray spectra with the 1T and 2T collisional plasma model APEC (Smith et al. 2001). The fitted parameters using these models were similar to those determined using the MEKAL model. For the star LO Peg there were two data sets corresponding to two observations. The spectrum was accumulated from each data set and fitted using the above-mentioned models individually, as well as jointly. The best-fit parameters were determined using the χ^2 minimization technique. These parameters were found to be similar in either case. Table 5 summarizes the best-fit values obtained for the various parameters along with the minimum $\chi^2_\nu = \chi^2/\nu$ (where ν is degrees of freedom) and the 90% confidence error bars estimated from the minimum $\chi^2 + 2.71$.

Single-temperature MEKAL models with abundances fixed to the solar values gave an unacceptably high value of χ^2_ν for both HD 95559 and LO Peg. However, 1T MEKAL models with abundances <0.02 times the solar abundances and with plasma temperatures in the range of 0.63–0.77 keV were found acceptable for HD 95559 but not for LO Peg. Two-temperature plasma models with the abundances fixed to the solar value were not found to be acceptable for either star. Acceptable MEKAL 2T fits were achieved when the abundances were allowed to depart from the solar values for both stars. The best-fit 2T plasma models with subsolar abundances along with the significances of the residuals in terms of their ratio for both HD 95559 and LO Peg are shown in the left and right panels of Figure 10. For HD 95559 an acceptable fit was obtained for abundances that were only $0.25^{+0.3}_{-0.2}$ times the solar values and with plasma components at temperatures of 0.45 and 1.27 keV. In the case of LO Peg the best-fit plasma temperatures were $0.30^{+0.04}_{-0.05}$ and $1.0^{+0.1}_{-0.2}$ keV,

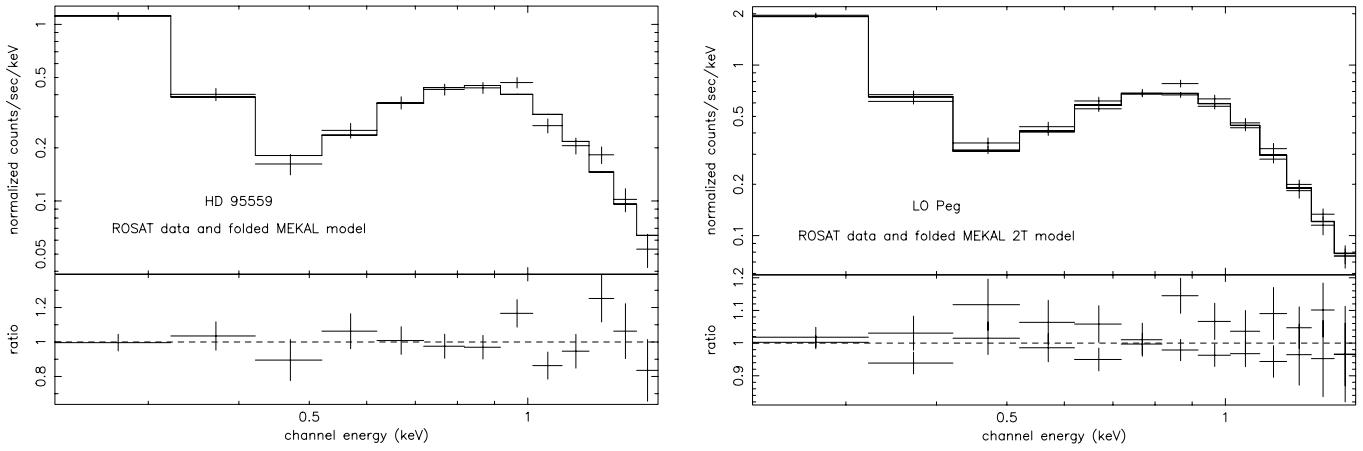

FIG. 10.—Spectrum of HD 95559 (*left*) and LO Peg (*right*) with the *ROSAT* PSPC, along with a 2T MEKAL model. The bottom plots in each panel represent the ratio of the observed counts to the counts predicted by the best-fit model.

TABLE 5
RESULTS OF X-RAY SPECTRAL ANALYSIS

Object	Model	Abundances[a]	N_H (10^{20} cm^{-2})	kT_1 (keV)	EM_1 (10^{52} cm^{-3})	kT_2 (keV)	EM_2 (10^{52} cm^{-3})	χ^2_ν	ν
HD 95559	MEKAL 1T	1.0 (fixed)	0.00	0.31	5.7	...	...	28.3	10
	MEKAL 1T	<0.02	0.6 ± 0.4	$0.69^{+0.08}_{-0.06}$	33.7^{+8}_{-7}	...	...	1.7	9
	MEKAL 2T	1.0 (fixed)	0.00	0.26	4.1	1.16	5.8	2.5	8
	MEKAL 2T	$0.25^{+0.3}_{-0.2}$	<0.45	$0.45^{+0.19}_{-0.18}$	$10.9^{+3.1}_{-2.1}$	$1.27^{+4.4}_{-0.5}$	$12.3^{+3.1}_{-4.9}$	1.6	7
LO Peg.....	MEKAL 1T	1.0 (fixed)	0.00	0.31	1.6	...	...	37.7	23
	MEKAL 1T	0.01	0.5	0.58	7.6	...	...	2.0	22
	MEKAL 2T	1.0 (fixed)	<0.1	$0.21^{+0.01}_{-0.02}$	0.91 ± 0.06	0.85 ± 0.04	0.93 ± 0.04	1.8	21
	MEKAL 2T	<0.15	<4.1	$0.30^{+0.04}_{-0.05}$	$2.5^{+1.0}_{-0.6}$	$1.0^{+0.1}_{-0.2}$	1.9 ± 0.1	1.3	20

NOTES.—Here $\chi^2_\nu = \chi^2/\nu$, where ν is degrees of freedom. Errors are with 90% confidence based on $\chi^2_{\rm min} + 2.71$. No errors or upper limits are derived when $\chi^2_\nu > 2$. The distance is 54.3 pc for HD 95559 and 25.1 pc for LO Peg.

[a] Common value of abundances for all the elements with respect to the solar photosphere values.

with abundances that were only <0.15 times the solar values for both plasma components.

7. X-RAY AND RADIO PROPERTIES: COMPARISON WITH SIMILAR SYSTEMS

A sample of 35 BY Draconis systems were studied spectroscopically with *ROSAT* by Dempsey et al. (1997), assuming that their coronae had solar abundances. The average value of the low-temperature (kT_1) and high-temperature (kT_2) components for these BY Draconis systems is 0.19 ± 0.03 and 1.31 ± 0.04 keV, respectively. The value of kT_1 derived using subsolar abundances for both HD 95559 and LO Peg (see Table 5) is found to be more than the mean value of the BY Draconis systems. Please note that the value of kT_1 derived using solar abundances (see Table 5) is found to be consistent with that of the average value for the other BY Draconis systems in Dempsey et al. (1997). However, a 2T plasma model using solar abundances failed to fit data with a high signal-to-noise ratio and gave an unacceptably high value of χ^2_ν for both stars. The values of kT_2 are, however, consistent with those of the other BY Draconis systems. The average volume emission measures EM_1 and EM_2 for the BY Draconis systems in Dempsey et al. (1997) are $1.4 \pm 0.4 \times 10^{52}$ and $7.6 \pm 2.9 \times 10^{52}$ cm^{-3}, respectively. The volume emission measure EM_1 for the star HD 95559 is found to be ~7 times more than the average value for BY Draconis systems. However, the value of EM_1 for LO Peg is consistent with that of the BY Draconis systems. The value of EM_2 of the star HD 95559 using subsolar abundances is consistent with those of the other BY Draconis systems. However, the value of EM_2 for LO Peg is ~2–3 times less than the average value of the other BY Draconis systems.

X-ray flux measurements exist for a sample of 248 chromospherically active binary systems (CABSs; Strassmeier et al. 1993). On the basis of SIMBAD[5] spectral classification and the catalog of CABSs, we have divided the sample into 101 dwarfs, 65 subgiants, and 82 giants and computed the average X-ray luminosity. For the sample of 101 dwarfs the average and the median X-ray luminosity ($\log L_X$) are 29.6 ± 0.7 and 29.63 ergs s^{-1}, respectively. The inferred $\log L_X$ for HD 95559, LO Peg, and FR Cnc is 30.3, 29.7, and 29.4–30.1, respectively, where L_X is in units of ergs s^{-1}, which are all close to the average value for active dwarf systems. The average and median X-ray luminosity for the 65 subgiants and the 82 giant active systems are found to be 30.8 ± 0.5 and 30.83, and 30.7 ± 0.7 and 30.8 ergs s^{-1}, respectively. This indicates that the evolved systems (subgiants and giants) are more X-ray luminous than the dwarf systems, as expected, since these stars have larger surface areas from which to radiate X-rays. Radio flux measurements exist for a sample of 226 CABSs (82 dwarfs, 64 subgiants, and 80 giants). The average and median $\log L_{\rm rad}$ for a sample of 82 dwarfs are 14.8 ± 0.7 and 14.9 ergs s^{-1} Hz^{-1}, respectively. LO Peg has been detected as a radio source of $(3.6 \pm 0.5) \times 10^{-26}$ ergs cm^{-2} s^{-1} Hz^{-1} (Condon et al. 1998). However, FR Cnc and HD 95559 do not have any radio observations. Using a distance of 25.1 pc, the radio luminosity ($\log L_{\rm rad}$) of LO Peg is found to be 15.43 ergs s^{-1} Hz^{-1}, which is again close to the typical value for BY Draconis systems.

8. SPECTRAL TYPE, TEMPERATURE, AND OTHER PHYSICAL PARAMETERS

The value of the total Galactic reddening $E(B - V)$ in the direction of FR Cnc is estimated from Schlegel et al. (1998) to be 0.03 mag. However, given that the *Hipparcos* parallax of this star implies a distance of only 33 pc, it is likely that its light suffers little if any reddening, and for the remaining discussion,

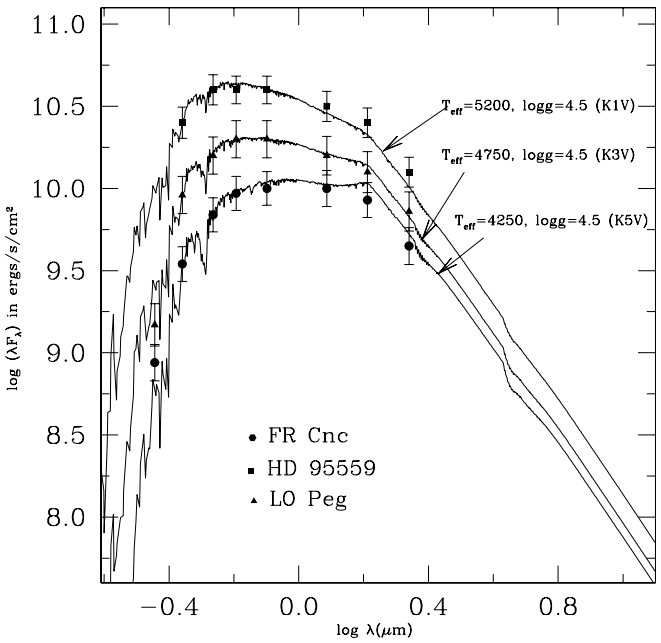

FIG. 11.—SEDs of the stars FR Cnc (*circles*), HD 95559 (*squares*), and LO Peg (*triangles*). The solid lines represent the model SEDs from R. L. Kurucz (1993, private communication) as expected from the intrinsic properties of the star. The vertical bars show the associated uncertainties due to the distance and the radius of the star.

[5] The SIMBAD database is operated at CDS, Strasbourg, France.

TABLE 6
PHYSICAL PARAMETERS OF FR CNC, HD 95559, AND LO PEG

Parameter	FR Cnc	HD 95559[a]	LO Peg
Spectral Type	K5 V	K1 V	K3 V
V	10.24 ± 0.01	8.93[b]	8.82 ± 0.01
M_V (mag)	7.60 ± 0.01	6.04	6.80 ± 0.01
M_{bol} (mag)	6.83 ± 0.01	5.67	6.30 ± 0.01
T_{eff} (K)	4250 ± 250	5250 ± 250	4750 ± 250
log g	4.5 ± 0.5	4.5 ± 0.5	4.5 ± 0.5
L ($L_\odot$)	0.13 ± 0.02	0.54 ± 0.03	0.25 ± 0.02
M ($M_\odot$)	0.60 ± 0.02	0.81 ± 0.01	0.66 ± 0.02
R ($R_\odot$)	0.70 ± 0.08	0.77 ± 0.10	0.72 ± 0.10
μ_α (mas yr^{-1})	-98.93 ± 1.99[b]	-140.79 ± 1.24[b]	132.06 ± 1.01[b]
μ_δ (mas yr^{-1})	-97.39 ± 1.44[b]	4.91 ± 0.87[b]	-144.83 ± 0.93[b]
π (mas)	30.24 ± 2.03[b]	18.43 ± 1.19[b]	39.91 ± 1.18[b]
R_V (km s^{-1})	27.0 ± 2.3,[c]	3.81 ± 0.11[d]	-17.4 ± 1.0
	24.0 ± 4.0[c]		

[a] Parameters are determined for an individual component of the binary system.
[b] *Hipparcos*.
[c] Upgren et al. (2002).
[d] Fekel & Henry (2000).

we assume $E(B-V) = 0.00$ mag. Using the *Hipparcos* parallax of 30.24 ± 2.03 mas and the value of $V = 10.24$ mag from our photometry, the absolute magnitude M_V of FR Cnc is 7.64 mag. (The *Hipparcos* V-band measurements and the V magnitude of Weis [1993] lead to similar values of $M_V = 7.7$ and 7.5 mag, respectively.) This value is consistent with a luminosity class V for this star. The color $(B-V)$ of FR Cnc derived from our photometry is 1.11 ± 0.02, compared to the redder but much lower precision value of 1.62 ± 0.20 given in the *Hipparcos* catalog. The 1.11 value of $(B-V)$ is best matched with a spectral class of K5 V. While this is three subclasses earlier than the spectral class K8 given in the *Hipparcos* catalog, the latter appears to be derived from a fairly crude spectral classification by Vyssotsky (1956), and thus the difference is likely not significant.

We have determined the spectral energy distribution (SED) of FR Cnc, HD 95559, and LO Peg using broadband *UBVRI* (present photometry and literature) and the Two Micron All Sky Survey (2MASS) *JHK* (Cutri et al. 2003) fluxes. We have assumed negligible reddening for each star. The observed SEDs of FR Cnc, HD 95559, and LO Peg are shown along with the synthetic SEDs (R. L. Kurucz 1993, private communication). The synthetic SEDs are predicted from the intrinsic properties of the stars. The model SEDs are shown in Figure 11.

The values of T_{eff} and log g that best match the observed SED are 4250 ± 250 K and 4.5 ± 0.5, respectively, and are consistent with the previously inferred K5 V spectral type for FR Cnc. The SED of HD 95559 (Fig. 11, *squares*) is well matched with the synthetic SED for a K1 V type star. This indicates that HD 95559 is a K1 V type star, as concluded by Fekel & Henry (2000). The SED of the star LO Peg is represented by filled triangles. Observations of LO Peg by Jeffries et al. (1994b) showed it to be a single K5–K7 dwarf, while Bowyer et al. (1996) had reported it to be a K8 type star. From the present photometry the absolute magnitude ($M_V = 6.8$) and color ($B-V = 1.04$) of the star LO Peg are consistent with a spectral type of K3 V. It is also clear from Figure 11 that the synthetic SED of a K3 V ($T_{eff} = 4750 \pm 250$ K; log $g = 4.5$) type star is well matched with the SED of LO Peg.

Using the *Hipparcos* parallax, the inferred T_{eff} and log g values, and various relations given in Landolt-Borstein (Schaifers & Voigt 1982), we have determined values of $M/M_\odot$, $R/R_\odot$, and $L/L_\odot$ for FR Cnc, HD 95559, and LO Peg. These well-determined parameters along with M_V and M_{bol} are given in Table 6.

9. 2MASS *JHK* PHOTOMETRY OF FR CNC, HD 95559, AND LO PEG

One of the most remarkable properties sometimes attributed to chromospherically active stars is the evidence of IR excesses, which is related to the properties of diffuse circumstellar matter (Scaltriti et al. 1993). Assuming negligible reddening and the 2MASS *JHK* magnitudes (Cutri et al. 2003), we have determined the intrinsic $(J-K)_0$ and $(H-K)_0$ for FR Cnc, HD 95559, and LO Peg. The intrinsic $(J-K)_0$ and $(H-K)_0$ colors are 0.77 and 0.16 mag for a K5 V type star and 0.54 and 0.11 mag for a K1 V type star (Koornneef 1983).

The intrinsic $(J-K)_0$ and $(H-K)_0$ colors of FR Cnc are 0.74 ± 0.03 and 0.14 ± 0.03 mag, implying a color excess of 0.03 ± 0.05 and 0.02 ± 0.03 mag in $(J-K)$ and $(H-K)$ color, respectively. The intrinsic $(J-K)_0 = 0.539 \pm 0.03$ and $(H-K)_0 = 0.111 \pm 0.03$ colors of HD 95559 give a color excess of 0.00 ± 0.03 in each $(J-K)$ and $(H-K)$ color. Assuming LO Peg to be a K3 V spectral type star, $(H-K)_0 = 0.69 \pm 0.03$ and $(J-K)_0 = 0.14 \pm 0.03$. The color excess in LO Peg is 0.02 ± 0.04 and 0.00 ± 0.03 mag, respectively. The values of the color excess for each star are consistent with zero to within the uncertainties, indicating that all three stars have no significant color excess in the *JHK* bands, which is also supported from the matching of the model SEDs, as shown in Figure 11.

10. KINEMATICS

We have computed the Galactic space velocity components (U, V, W) for the star FR Cnc from the proper motion and parallax measured by *Hipparcos* and the radial velocities measured by Upgren et al. (2002) as listed in Table 6. The resulting values and their associated errors are given in Table 7.

FR Cnc, HD 95559, and LO Peg are inside the boundaries for the young disk population in the (U, V) and (W, V) diagrams (Montes et al. 2001). The (U, V, W) components of FR Cnc are close to those of the IC 2391 supercluster $(-20.6, -15.7, -9.1)$, which is estimated to have an age of 35–55 Myr and for which several dozen possible late-type members have been previously

TABLE 7
GALACTIC SPACE-VELOCITY COMPONENTS

Star	$R_V \pm \sigma_{R_V}$	$U \pm \sigma_U$	$V \pm \sigma_V$	$W \pm \sigma_W$	$V_{total} \pm \sigma_{V_{total}}$
FR Cnc	27.0 ± 2.3	-25.2 ± 1.7	-23.4 ± 0.9	-4.3 ± 1.4	34.7 ± 2.0
	24.0 ± 4.0	-23.0 ± 3.1	-22.2 ± 1.7	-5.7 ± 2.2	32.5 ± 3.7
HD 95559	3.81 ± 0.11	-32.9 ± 0.4	-10.9 ± 0.2	-11.2 ± 0.1	36.4 ± 05
LO Peg	-17.4 ± 1.0	-5.2 ± 0.29	-23 ± 0.95	-23.86 ± 0.95	29.0

NOTE.—All units are km s^{-1}.

identified. The star LO Peg has also been identified as a young star previously: as a member of either the 100 Myr old Local Association (Montes et al. 2001) or the 50 Myr old AB Dor moving group (Zuckerman et al. 2004). We have also calculated the (U, V, W) components for HD 95559 using the radial velocity 3.81 ± 0.11 km s^{-1} (Fekel & Henry 2000) and the parallax and proper motion given in the *Hipparcos* catalog. The (U, V, W) components of this star (see Table 7) indicate that it is a possible member of the 600 Myr old Hyades supercluster, although, as already noted, its strong Li I absorption lines are more consistent with a Pleiades-type age of 100 Myr.

11. SUMMARY AND CONCLUSIONS

The shape and amplitude of the photometric light curves of FR Cnc, HD 95559, and LO Peg are observed to be changing from one epoch to another. The change in the amplitude is mainly due to a change in the minimum of the light curve, and this may be due to a change in the spot coverage. This indicates the BY Draconis type of variability in these dwarf systems. In such late types of dwarfs, convection and rapid rotation generate a dynamo, resulting in starspot activity. Two groups of spots are identified for FR Cnc and LO Peg. The spots are found to migrate, and migration periods of 0.97 and 0.93 yr are determined from the 4 years of data. A migration period of 1.12 yr for one group of spots in LO Peg is also determined. A new group of spot formation in the star HD 95559 was seen during our observations. We determine the spectral types of FR Cnc and LO Peg to be K5 V and K3 V, respectively.

Long-term optical photometry of FR Cnc firmly establishes the rotation period of the star to be 0.8267 days. Variable Hα, Hβ, and Ca II H and K emission in the spectra of FR Cnc indicate the presence of a heated atmosphere outside the photosphere. The chromospheric line emission seems to correlate with the photometric light curve, i.e., maximum at the light curve minimum or minimum at the light curve maximum. The excess emission-line ratio of FR Cnc implies that this emission likely arises from an extended region rather than from plages or prominences. The X-ray spectral parameters of HD 95559 and LO Peg are found to be consistent with those of other BY Draconis type systems.

The bulk of the optical, X-ray, and kinematical data indicate that these three stars are all active, young stars of 100 Myr or less, whose high activity levels are primarily due to their youth. HD 95559 is particularly interesting in that it is both young and a synchronized close binary system, whose current rapid rotation is expected to persist for many gigayears, and it is remarkably similar to another young synchronized binary system, V824 Ara (HD 155555; see, e.g., Strassmeier & Rice 2000). We believe that this study has reconfirmed that selecting stars by their high X-ray-to-optical flux ratios is an efficient way to identify young active stars in the solar neighborhood.

We are grateful to the referee Graham M. Harper for valuable comments and suggestions. We are thankful to the time allocation committee for giving time at the 234 cm VBT. We are also thankful to Brijesh Kumar for useful discussions on the optical spectroscopic aspects of the work. This research has made use of data obtained from HEASARC, provided by the NASA Goddard Space Flight Center. Starlink is funded by PPARC and based at the Rutherford Appleton Laboratory, which is part of the Council for the Central Laboratory of the Research Councils, UK. This publication makes use of data products from 2MASS, which is a joint project of the University of Massachusetts and the Infrared Processing and Analysis Center, California Institute of Technology, funded by the National Aeronautics and Space Administration and the National Science Foundation.

REFERENCES

Anders, E., & Grevesse, N. 1989, Geochim. Cosmochim. Acta, 53, 197
Ayres, T. R., et al. 1995, ApJS, 96, 223
Bailer-Jones, C. A. L., & Mundt, R. 2001, A&A, 367, 218
Barnes, J. R., Collier Cameron, A., James, D. J., & Steeghs, D. 2001, MNRAS, 326, 1057
Bopp, B. W. 1987, ApJ, 317, 781
Bopp, B. W., & Fekel, F., Jr. 1977, AJ, 82, 490
Bopp, B. W., Noah, P. V., Klimke, A., & Africano, J. 1981, ApJ, 249, 210
Bopp, B. W., & Stencel, R. E. 1981, ApJ, 247, L131
Bos, M. 1994, Inf. Bull. Variable Stars, 4111, 1
Bowyer, S., Lampton, M., Lewis, J., Wu, X., Jelinsky, P., & Malina, R. F. 1996, ApJS, 102, 129
Caillault, J.-P., Drake, S. A., & Florkowski, D. R. 1988, AJ, 95, 887
Condon, J. J., Cotton, W. D., Greisen, E. W., Yin, Q. F., Perley, R. A., Taylor, G. B., & Broderick J. J. 1998, AJ, 115, 1693
Cutri, R. M., et al. 2003, 2MASS All-Sky Catalogue of Point Sources (Pasadena: IPAC)
Dal, H. A., & Tas, G. 2003, Inf. Bull. Variable Stars, 5390, 1
Dempsey, R. C., Linsky, J. L., Fleming, T. A., & Schmitt, J. H. M. M. 1997, ApJ, 478, 358
Dempsey, R. C., Linsky, J. L., Schmitt, J. H. M. M., & Fleming, T. A. 1993, ApJ, 413, 333
Donati, J.-F., & Collier Cameron, A. 1997, MNRAS, 291, 1
Drake, S. A., Simon, T., & Linsky, J. L. 1989, ApJS, 71, 905
———. 1992, ApJS, 82, 311
Eibe, M. T., Byrne, P. B., Jeffries, R. D., & Gunn, A. G. 1999, A&A, 341, 527
Elvis, M., Plummer, D., Schachter, J., & Fabbiano, G. 1992, ApJS, 80, 257
Fekel, F. C., & Henry, G. W. 2000, AJ, 120, 3265
Fekel, F. C., Moffett, T. J., & Henry, G. W. 1986, ApJS, 60, 551
Glebocki, R., & Stawikowski, A. 1997, A&A, 328, 579
Güdel, M., Schmitt, J. H. M. M., Bookbinder, J. A., & Fleming, T. A. 1993, ApJ, 415, 236
Hall, D. S. 1976, in IAU Colloq. 29, Multiple Periodic Variable Stars, ed. W. S. Fitch (Dordrecht: Reidel), 387
Hall, J. C., & Ramcey, L. W. 1992, AJ, 104, 1942
Innis, J. L., Coates, D. W., Thompson, K., & Lloyd Evans, T. 1990, MNRAS, 242, 306
Jeffries, R. D., Bertram, D., & Spurgeon, B. R. 1994a, Inf. Bull. Variable Stars, 4091, 1
Jeffries, R. D., Byrne, P. B., Doyle, J. G., Anders, G. J., James, D. J., & Lanzafame, A. C. 1994b, MNRAS, 270, 153
Jeffries, R. D., & Jewell, S. J. 1993, MNRAS, 264, 106
Kazarovets, A. V., Samus, N. N., Durlevich, O. V., Frolov, M. S., Antipin, S. V., Kireeva, N. N., & Pastukhova, E. N. 1999, Inf. Bull. Variable Stars, 4659, 1
Koornneef, J. 1983, A&A, 128, 84
Landolt, A. U. 1992, AJ, 104, 340
Liedahl, D. A., Osterheld, A. L., & Goldstein, W. H. 1995, ApJ, 438, L115
Mewe, R., Kaastra, J. S., & Liedahl, D. A. 1995, Legacy, 6, 16
Montes, D., López-Santiago, J., Gálvez, M. C., Fernández-Figueroa, M. J., De Castro, E., & Cornide, M. 2001, MNRAS, 328, 45
Morris, D. H., & Mutel, R. L. 1988, AJ, 95, 204
Morrison, R., & McCammon, D. 1983, ApJ, 270, 119
Padmakar, Singh, K. P., Drake, S. A., & Pandey, S. K. 2000, MNRAS, 314, 733
Pandey, J. C., Singh, K. P., Sagar, R., & Drake, S. A. 2002, Inf. Bull. Variable Stars, 5351, 1
Perryman, M. A. C., et al. 1997, A&A, 323, L49
Pfeffermann, E., et al. 1987, Proc. SPIE, 733, 519
Raveendran, A. V., & Mohin, S. 1995, A&A, 301, 788
Robb, R. M., & Cardinal, R. D. 1995, Inf. Bull. Variable Stars, 4221, 1
Roberts, D. H., Lehar, J., & Dreher, J. W. 1987, AJ, 93, 968
Scaltriti, F., Busso, M., Ferrari-Toniolo, M., Origlia, L., Persi, P., Robberto, M., & Silvestro, G. 1993, MNRAS, 264, 5
Schachter, J. F., Remillard, R., Saar, S. H., Favata, F., Sciortino, S., & Barbera, M. 1996, ApJ, 463, 747
Schaifers, K., & Voigt, H. H. 1982, Numerical Data and Functional Relationships in Science and Technology, New Series, Group VI, Vol. 2b (Berlin: Springer)
Schlegel, D. J., Finkbeiner, D. P., & Davis, M. 1998, ApJ, 500, 525

Smith, R. K., Brickhouse, N. S., Liedahl, D. A., & Raymond, J. C. 2001, ApJ, 556, L91
Strassmeier, K. G., Hall, D. S., Fekel, F. C., & Scheck, M. 1993, A&AS, 100, 173
Strassmeier, K. G., & Rice, J. B. 2000, A&A, 360, 1019
Strassmeier, K. G., Washuettl, A., Granzer, T., Scheck, M., & Weber, M. 2000, A&AS, 142, 275
Trümper, R. A. 1983, Adv. Space Res., 2, 241
Upgren, A. R., Sperauskas, J., & Boyle, R. P. 2002, Baltic Astron., 11, 91
Voges, W., et al. 1999, A&A, 349, 389
Vyssotsky, A. N. 1956, AJ, 61, 201
Weis, E. W. 1993, AJ, 105, 1962
Zuckerman, B., Song, I., & Bessel, M. S. 2004, ApJ, 613, L65